Article

Discovery Medicine 2025; 37(201): 2320–2333
https://doi.org/10.24976/Discov.Med.202537201.197

EPA-Induced Gut Microbiota Remodeling Restores Mitochondrial Function and Enhances Efferocytosis to Combat Atherosclerosis

Yiqiu Zhou[1], Si Chen[2], Jianing Li[1], Decai Zhu[2,*]

[1]Department of Clinical Nutrition, The First Affiliated Hospital of Ningbo University, 315020 Ningbo, Zhejiang, China
[2]Cardiology Department, The First Affiliated Hospital of Ningbo University, 315020 Ningbo, Zhejiang, China
*Correspondence: ndfyzhudecai@sina.com (Decai Zhu)
Submitted: 23 July 2025 Revised: 13 August 2025 Accepted: 27 August 2025 Published: 20 October 2025

Background: Eicosapentaenoic acid (EPA) effectively modulates immune responses and reshapes the gut microbiota. Therefore, this study aims to investigate the role of EPA in modulating the composition of gut microbial and restoring mitochondrial and efferocytic function in atherosclerosis (AS).

Methods: Male apolipoprotein E knockout (ApoE$^{-/-}$) mice were fed a high-fat diet to induce AS and then subjected to EPA treatment. Fecal microbiota transplantation (FMT) was performed using fecal samples from untreated AS mice. Histopathological changes in the aortic root were assessed using hematoxylin and eosin staining and Oil Red O staining approaches. Serum lipid profiles were quantified using corresponding biochemical assays. Mitochondrial membrane potential and reactive oxygen species (ROS) levels were evaluated using 5,5′,6,6′-Tetrachloro-1,1′,3,3′-tetraethyl-imidacarbocyanine iodide (JC-1) and 2′,7′-dichlorofluorescein diacetate (DCFH-DA) staining, respectively. Efferocytosis was analyzed using Diff-Quick staining, and the composition and functions of the gut microbiota were analyzed using 16S rRNA gene sequencing.

Results: EPA treatment attenuated AS progression and improved serum lipid profiles by reducing total cholesterol (TC), triglycerides (TG), and low-density lipoprotein cholesterol (LDL-C) while increasing high-density lipoprotein cholesterol (HDL-C). Furthermore, EPA treatment restored mitochondrial membrane potential, reduced ROS production, and enhanced macrophage efferocytosis in the aorta. Microbial analysis revealed that EPA reshaped the composition of gut microbiota by enriching beneficial bacterial taxa and altering metabolic pathways, including those related to carbohydrate metabolism and xenobiotic degradation. Notably, FMT from AS mice effectively reversed the protective effects of EPA on mitochondrial function, ROS levels, and efferocytosis.

Conclusion: This study demonstrates that EPA alleviates atherosclerotic pathology by modulating the composition of gut microbiota, restoring mitochondrial function, and enhancing efferocytosis. The findings support the therapeutic potential of EPA as a microbiota-targeting intervention for cardiovascular disease.

Keywords: eicosapentaenoic acid; atherosclerosis; gut microbiota; mitochondrial dysfunction; efferocytosis

Introduction

Atherosclerosis (AS) is a chronic, progressive vascular disease characterized by abnormalities in lipid metabolism, persistent inflammation, and vascular endothelial dysfunction [1]. Pathologically, it is implicated as lipid deposition beneath the arterial intima, infiltration of inflammatory cells, formation of fibrous caps, and progressive narrowing or occlusion of the arterial lumen. These pathological alterations comprise coronary, cerebral, and peripheral arteries, resulting in cardiovascular and cerebrovascular events [2]. Epidemiological evidence indicates that AS and its complications remain among the leading causes of morbidity and mortality worldwide, with increasing incidence and mortality rates, particularly in middle-aged and elderly populations, posing a significant threat to public health and quality of life [3]. Elucidating the molecular mechanisms of AS and identifying key regulatory factors and signaling pathways are essential for developing novel therapeutic approaches.

Dysfunctional efferocytosis, a crucial homeostatic mechanism responsible for clearing dead cells and resolving inflammation [4], is increasingly recognized as a key driver of atherosclerosis. Evidence indicates that enhancing macrophage-mediated efferocytosis can significantly inhibit the accumulation of foam cells, reduce plaque-associated inflammation, and thus delay the progression of AS [5]. The “health status” of mitochondria is closely linked to efferocytosis through autophagy, as restoring mitochondrial function and inhibiting the accumulation of damaged mitochondria are critical to maintaining effective immune clearance [6]. Furthermore, disruption of the

gut microbiota has been reported to impair mitochondrial metabolic pathways in intestinal epithelial cells, thereby disturbing intestinal homeostasis [7]. Additionally, gut microbiota has been reported to influence the progression of AS by regulating genes involved in efferocytosis [8]. Furthermore, certain probiotics and their metabolites can play a protective role against AS by improving mitochondrial function [9]. Notably, previous research has shown that the ketone body 3-hydroxybutyrate (3-HB) can alleviate systemic inflammation and delay AS progression by reducing Ca^{2+} release from the endoplasmic reticulum to the mitochondria [10].

Eicosapentaenoic acid (EPA), a key omega-3 polyunsaturated fatty acid primarily derived from deep-sea fish oil, possesses diverse biological properties, including anti-inflammatory, lipid-lowering, antiplatelet aggregation, and cardiometabolic regulatory effects [11]. In cardiovascular health, EPA alleviates endothelial dysfunction induced by saturated fatty acids and supports endothelial homeostasis by preserving mitochondrial integrity [12]. Additionally, EPA-derived resolvin E4 promotes macrophage-mediated clearance of apoptotic cells [13]. Emerging evidence further highlights EPA's significant role in modulating the gut microbiota [14]. EPA-enriched phosphatidylethanolamine plasmalogens can reshape gut microbiota and regulate bile acid metabolism, ultimately attenuating atherosclerotic lesions in low-density lipoprotein receptor (LDLR)-deficient mice [15]. These observations suggest that EPA may reduce mitochondrial dysfunction by reshaping gut microbiota, subsequently enhancing the efferocytosis of macrophages and ultimately delaying the progression of AS.

Based on these findings, this study comprehensively investigated the regulatory effects of EPA on gut microbiota composition and mitochondrial function, elucidating its potential protective mechanisms in AS progression. These insights provide both theoretical and experimental support for developing EPA-based therapeutic strategies to prevent AS.

Materials and Methods

Animal Ethics

Male C57BL/6J apolipoprotein E knockout ($ApoE^{-/-}$) mice (n = 36), aged 6 weeks and weighing 18–22 g, were purchased from Viewsolid Biotech (China). All animal procedures were approved by the Institutional Animal Care and Use Committee of Zhejiang Baiyue Biotechnology Co., Ltd. (ZJBYLA-IACUC-20240715) and conducted in compliance with the Guide for the Care and Use of Laboratory Animals. The mice were housed in a specific pathogen-free (SPF) facility under a controlled environment of a 12-h light/dark cycle, 22 ± 2 °C temperature, 50 ± 5% relative humidity, and unlimited access to food and water.

Animal Grouping and Treatment

Mice were randomly assigned (n = 6 per group) into three groups (n = 6 per group): Control, AS, and AS+EPA (Group 1). Mice in the Control group received a standard chow diet (D12450B; TROPHIC Animal Feed High-Tech Co., Ltd., Nantong, China), while the AS and AS+EPA groups were fed a high-fat diet (HFD, D12492; TROPHIC Animal Feed High-Tech Co., Ltd., Nantong, China) to induce AS modeling [16]. In the AS+EPA group, EPA (4 g/kg/day, 2.5% w/w; HY-B0660, MCE, Monmouth Junction, NJ, USA) was administered orally [17]. Furthermore, mice in the AS and Control groups received an equivalent volume of physiological saline (ST341, Beyotime, Shanghai, China). After a 12-week treatment course, fresh fecal samples were obtained for sequencing and further analysis.

For the fecal microbiota transplantation (FMT) experiment, mice were randomly divided into AS, AS+EPA, and AS+EPA+FMT groups (Group 2), with 6 animals per group. Mice in the AS group were fed a high-fat diet (HFD) for 12 weeks. Starting from week 10, they received 200 µL of normal saline by gavage (once daily) for 2 weeks. The AS+EPA group was fed an HFD for 12 weeks while simultaneously receiving 2.5% (w/w) EPA (4 g/kg/d; suspension in corn oil, HY-B0747, MedChemExpress, Shanghai, China) for 12 weeks. Similarly, from week 10, these mice also received 200 µL of normal saline by gavage once a day for 2 weeks. Mice in the AS+EPA+FMT group were fed an HFD for 12 weeks while simultaneously taking 2.5% (w/w) EPA (4 g/kg/d) for 12 weeks [18]. Starting from week 10, they were treated with FMT supernatant (200 µL) by gavage once a day for 2 weeks. The FMT supernatant was prepared by combining 200 mg of fresh fecal pellets from the AS mice (Group 1) in 5 mL of sterile saline, vortexing vigorously for 3 minutes, and allowing the suspension to settle by gravity for 2 minutes. The resulting supernatant was collected and administered daily for two weeks.

Following the 12-week treatment course, mice were anesthetized with 4% isoflurane (26675-46-7, Sangon, Shanghai, China), and blood samples were collected via retro-orbital puncture. The mice were then euthanized by cervical dislocation, and the aortic root was collected. Furthermore, reactive oxygen species (ROS) and mitochondrial membrane potential were assessed in portions of fresh tissue. Remaining tissue samples were snap-frozen in liquid nitrogen and stored at –80 °C for further analyses, whereas selected samples were fixed in 4% paraformaldehyde (P0099, Beyotime, Shanghai, China) for histological examination.

Histological Analysis

Aortic root tissues were fixed in paraffin (8002-74-2; Nanjing Reagent, Nanjing, China), and sectioned for histological examination. Sections were stained using either Oil Red O (C0157, Beyotime, Shanghai, China) or

Hematoxylin and Eosin (H&E; C0105, Beyotime, Shanghai, China), following the manufacturer's instructions.

For the Oil Red O assay, sections were briefly rinsed in 60% isopropanol and then stained with a freshly prepared and filtered Oil Red O working solution for 15–20 minutes at room temperature. After thoroughly washing with distilled water, sections were counterstained with a hematoxylin staining solution (C0107, Beyotime, Shanghai, China) for 1–2 minutes. After a final wash with distilled water, sections were mounted using mounting medium (P0126, Beyotime, Shanghai, China).

For the H&E assay, sections were stained with Harris Hematoxylin solution for 5–8 minutes, soaked in distilled water to remove excess stain, and then counterstained with Eosin Y solution for 1–3 minutes. Finally, the sections were mounted with neutral balsam (C0173, Beyotime, Shanghai, China).

All the prepared slides were examined, and images were captured using a Nikon Eclipse 80i optical microscope (200× and 400× magnifications; Nikon, Tokyo, Japan).

Serum Lipid Measurements

Whole blood samples were centrifuged to collect serum, which was then analyzed for lipid parameters using commercial assay kits, including triglycerides (TG; CB10296-Mu, Coibo, Shanghai, China), total cholesterol (TC; CB10869-Mu, Coibo, Shanghai, China), high-density lipoprotein cholesterol (HDL-C; CB10316-Mu, Coibo, Shanghai, China), and low-density lipoprotein cholesterol (LDL-C; D721158-0048, Sangon, Shanghai, China), following the manufacturer's instructions. Finally, absorbance was measured at 450 nm using a microplate reader (Bio-Rad, Hercules, CA, USA).

Mitochondrial Membrane Potential

The mitochondrial membrane potential was assessed using a 5,5',6,6'-Tetrachloro-1,1',3,3'-tetraethylimidacarbocyanine iodide (JC-1) Mitochondrial Membrane Potential Assay Kit (C2006, Beyotime, Shanghai, China) and a Tissue Mitochondria Isolation Kit (C3606, Beyotime, Shanghai, China). Briefly, mitochondria were isolated from fresh aortic root tissue and incubated with the JC-1 working solution for 30 minutes. Fluorescence was then examined using a fluorescence microscope (DM1000, Leica, Shanghai, China), where red fluorescence indicated a high membrane potential and green fluorescence represented a low membrane potential. Finally, images were analyzed using ImageJ software (NIH, Bethesda, MD, USA).

Evaluation of ROS Levels

Fresh aortic root tissues were washed with cold phosphate-buffered saline (PBS; C0221A, Beyotime, Shanghai, China), minced, and then enzymatically digested with trypsin (40101ES25, Yeasen, Shanghai, China) to obtain single-cell suspensions. Suspensions were filtered through a cell strainer (J00070, SHJASW, Shanghai, China), resuspended in PBS, and then incubated with 10 μM 2′,7′-dichlorofluorescein diacetate (DCFH-DA; S0033S, Beyotime, Shanghai, China) for 30 minutes. ROS fluorescence was then detected using flow cytometry (Agilent Technologies, Santa Clara, CA, USA).

Diff-Quick Staining

The paraffin-embedded aortic root tissues were sectioned and then stained using a Diff-Quick Stain Kit (40748ES60, Yeasen, Shanghai, China). Images were recorded under an optical microscope at 100× or 200× magnification. Apoptotic bodies appeared as purplish-red granules, with cytoplasm stained light blue or pink and nuclei dark blue. The phagocytosis rate (%) was determined using the following formula. Phagocytosis rate (%) = (Number of cells containing ingested apoptotic cells/Total number of cells) × 100.

16S rRNA Gene Sequencing and Analysis

Genomic DNA was extracted from mouse fecal samples using the DNeasy PowerLyzer PowerSoil Kit (QIA12855, Qiagen, Shanghai, China), following the manufacturer's instructions. For each sample, 30 ng of high-quality genomic DNA was amplified by PCR using fusion primers. PCR products were purified with Agencourt AMPure XP magnetic beads, eluted in buffer, and then prepared for library construction. Library concentration and size distribution were assessed using an Agilent 2100 Bioanalyzer (Agilent Technologies, Santa Clara, CA, USA). Qualified libraries were then sequenced employing the Illumina HiSeq platform (Illumina, USA) according to insert size specifications.

Sequence data were aligned to the 16S rRNA reference database (v138) and processed using the Quantitative Insights into Microbial Ecology 2 (QIIME2, V. 2.0.2) workflow. The Divisive Amplicon Denoising Algorithm 2 (DADA2) was used for quality control and denoising. Forward and reverse reads were terminated at 240 and 180 bp, respectively. Operational taxonomic units (OTUs) were clustered at 97% similarity, and taxonomic classification from kingdom to species level was performed using the SILVA full-length 16S rRNA classifier. Furthermore, rarefaction curves were generated using the vegan (V. 2.6-8) and phyloseq (V. 1.49.0) packages in R software (V. 4.1.2). Downstream analyses, such as alpha diversity estimate were conducted using microbiotaProcess (V. 1.17.1), treeio (V. 1.26.0), and microeco (V. 1.9.1). Beta diversity was assessed using the Bray-Curtis distance and the Adonis test, with the results expressed through principal coordinate analysis (PCoA). Differential taxa analysis was performed using microeco (V. 1.9.1), and significant variations in relative abundance across taxonomic levels were evaluated using linear discriminant analysis effect size (LEfSe).

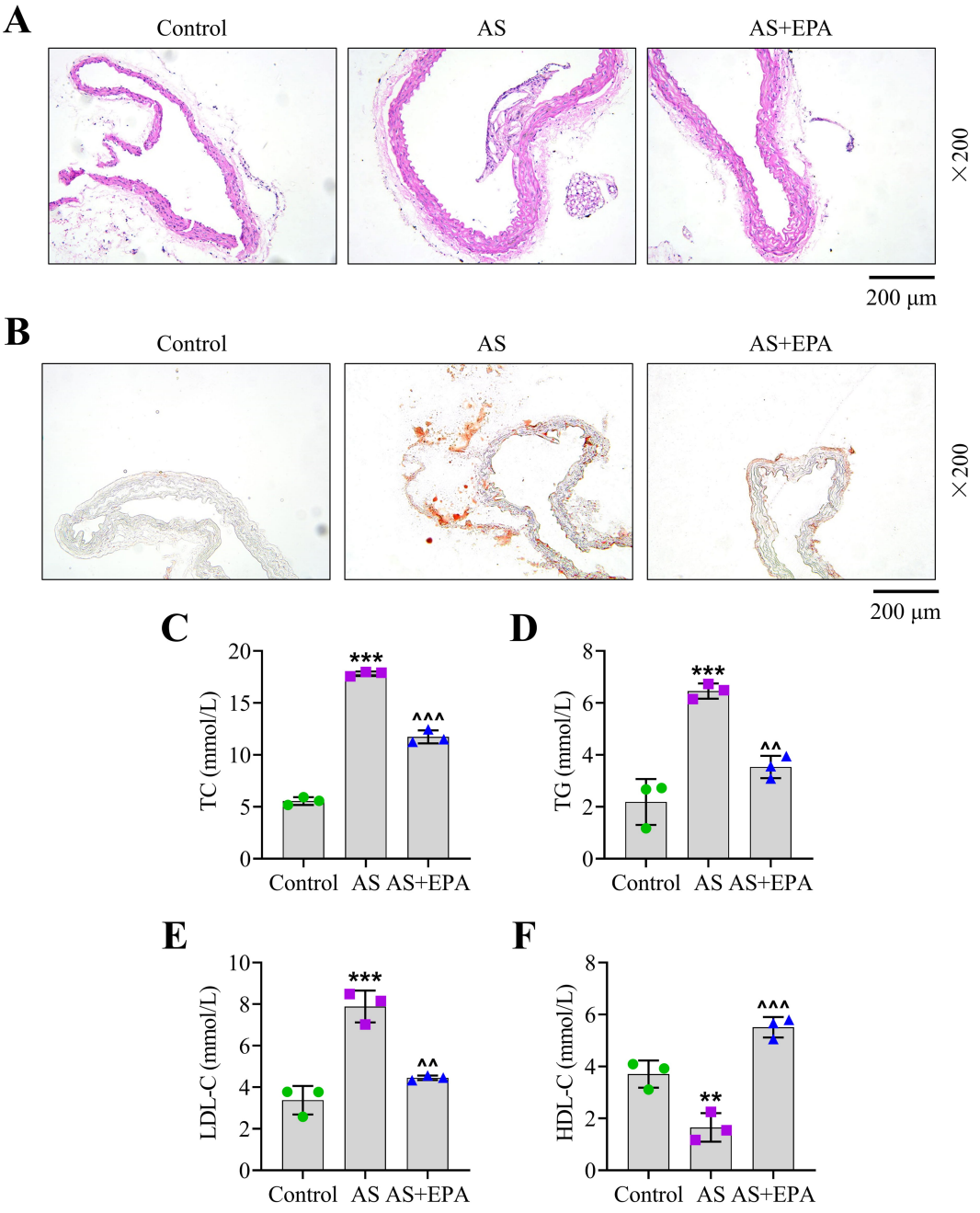

Fig. 1. Eicosapentaenoic acid (EPA) regulates histopathological changes and lipid markers in atherosclerosis (AS). (A,B) Hematoxylin and eosin (H&E) staining (A) and Oil Red O staining (B) showed histopathological changes in the aortic root of the Control, AS, and AS+EPA groups. Magnification: 200×; scale bar: 200 μm. (C–F) Serum levels of triglycerides (TG), total cholesterol (TC), high-density lipoprotein cholesterol (HDL-C), and low-density lipoprotein cholesterol (LDL-C) were assessed in the Control, AS, and AS+EPA groups using commercial kits. n = 3 per group. $^{**}p < 0.01$, $^{***}p < 0.001$ versus Control; $^{\wedge\wedge}p < 0.01$, $^{\wedge\wedge\wedge}p < 0.001$ versus AS.

Furthermore, PICRUSt2 (V. 2.4.1) was applied to perform functional profiling of the gut microbiota based on 16S rRNA gene sequences, enabling the identification of Kyoto Encyclopedia of Genes and Genomes (KEGG) level 2 metabolic pathways and evaluation of functional differences among groups.

Statistical Analysis

Statistical analysis was conducted using GraphPad 8.0 software (GraphPad Software Inc., San Diego, CA, USA). Data were expressed as mean ± standard deviation (SD). Differences among multiple groups were evaluated using one-way analysis of variance (ANOVA) followed by Tukey's post hoc test. A *p*-value of less than 0.05 was considered statistically significant.

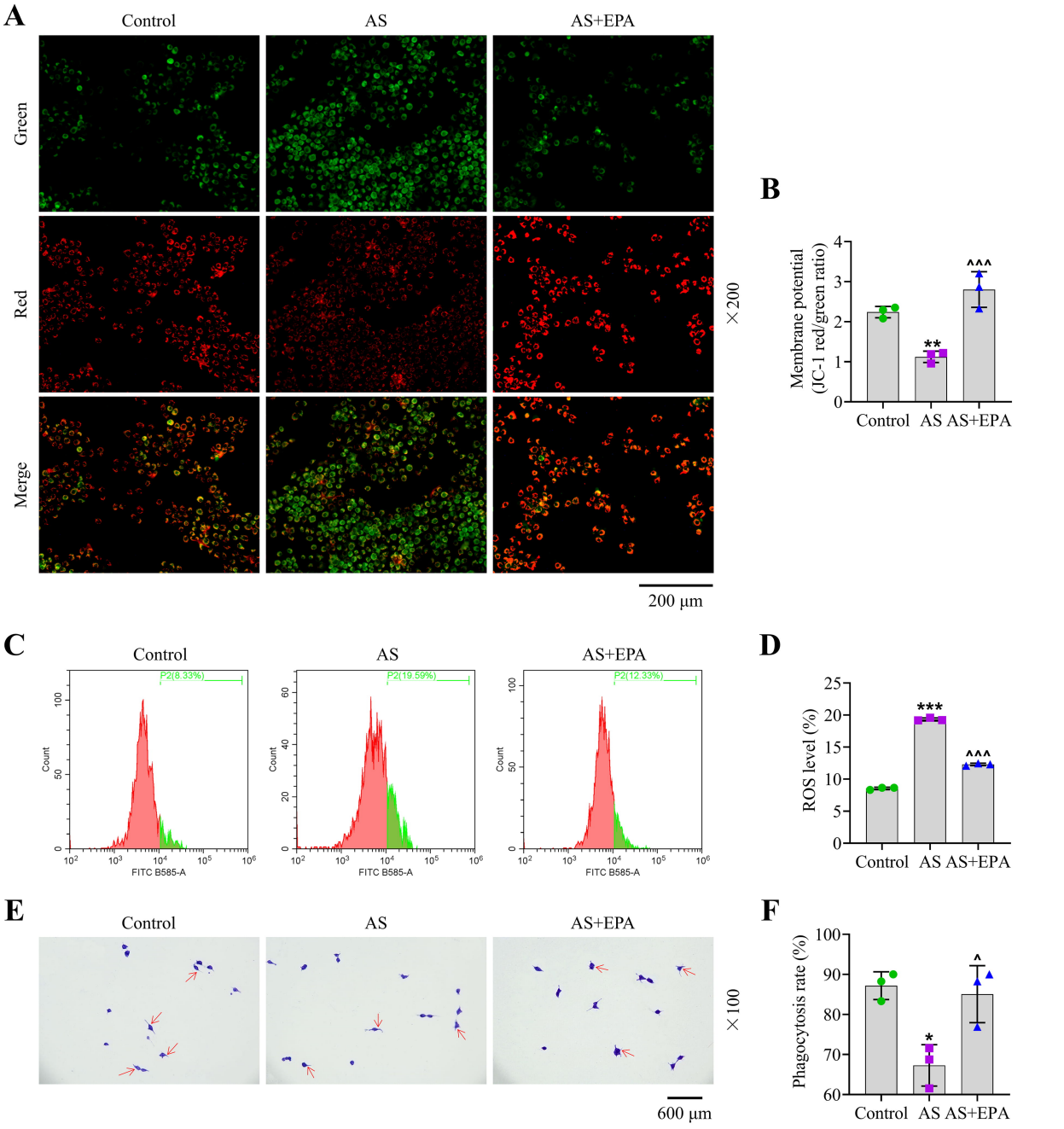

Fig. 2. EPA mediates mitochondrial membrane potential, reactive oxygen species (ROS) levels, and efferocytosis in AS. (A,B) Mitochondrial membrane potential in the aortic cells from the Control, AS, and AS+EPA groups was evaluated using the 5,5',6,6'-Tetrachloro-1,1',3,3'-tetraethyl-imidacarbocyanine iodide (JC-1) fluorescent probe assay. Magnification: 200×; scale bar: 200 μm. (C,D) ROS levels in the aortic cells were determined with 2′,7′-dichlorofluorescein diacetate (DCFH-DA) staining and flow cytometry in the Control, AS, and AS+EPA groups. (E,F) Diff-Quick staining was applied to assess efferocytosis in the aortic root of the Control, AS, and AS+EPA groups. Magnification: 100×; scale bar: 600 μm, arrows indicate the ingested apoptotic cells. n = 3 per group. $^{*}p < 0.05$, $^{**}p < 0.01$, $^{***}p < 0.001$ versus Control; $^{\wedge}p < 0.05$, $^{\wedge\wedge\wedge}p < 0.001$ versus AS.

Results

EPA Attenuates AS Progression by Restoring Mitochondrial Function and Enhancing Efferocytosis

H&E staining revealed classic atherosclerotic plaque lesions and a significant thickening of the aortic root vascular wall in the AS group (Fig. 1A). Oil Red O staining confirmed significant lipid deposition, as evidence by numerous red lipid droplets within the plaques in the AS group (Fig. 1B). Conversely, EPA therapy drastically attenuated vascular damage in the aortic root of AS mice (Fig. 1A,B).

Serum TC, TG, and LDL-C levels were substantially increased, and HDL-C levels were decreased following HFD feeding ($p < 0.01$, Fig. 1C–F). However, these changes were significantly alleviated by EPA intervention ($p < 0.01$, Fig. 1C–F). Mitochondrial assessment revealed that the AS group showed lower levels compared to the Control group ($p < 0.01$, Fig. 2A–D), while opposite trends were observed in the AS+EPA group relative to the AS group ($p < 0.001$, Fig. 2A–D).

Furthermore, efferocytosis in the aortic root was disrupted in AS mice, as evidenced by the reduced number of apoptotic cells ingested. However, EPA administration enhanced efferocytosis, as evidenced by a significant increase in apoptotic cell uptake ($p < 0.05$, Fig. 2E,F).

EPA Modulates Gut Microbiota Composition in Atherosclerotic Mice

To investigate the impact of EPA on gut microbiota, 16S rRNA sequencing was performed. Alpha diversity analysis unveiled that the ACE and Chao indices were significantly reduced in the AS group compared with the Control group ($p < 0.05$, Fig. 3A,C). Notably, there was no significant difference in the Shannon and Simpson index between the AS or EPA groups, compared with the control group (Fig. 3B,D). These results showed that the AS successfully induced a decrease in microbial community richness while maintaining the relative stability of the community structure. EPA treatment failed to significantly reverse the AS-induced decrease in richness and may have exerted a new reshaping effect on the microbial community structure. The trend suggests that it might have reduced the evenness of the community. However, beta diversity analysis revealed distinct clustering of the microbial communities among the Control, AS, and EPA groups, suggesting treatment-dependent differences in microbial composition (Fig. 3E), indicating both the AS and EPA treatments have changed the composition of the microbiota.

Relative abundance profiling at the phylum and genus levels (Fig. 4) demonstrated that Bacillota, Bacteroidota, Verrucomicrobiota, Pseudomonadota, Campylobacterota, and Actinomycota were dominant phyla. At the genus level, *Akkermansia* and *Helicobacter* were both increased, while *Muribaculum* and *Duncaniella* were decreased in the AS and EPA groups. Furthermore, the decrease in *Corynebacterium* and the increase in *Flintibacter* found in the AS group were partially reversed by EPA.

To identify microbial taxa contributing to these differences, LEfSe analysis was performed, demonstrating multiple taxonomic branches with significant differences among the three groups (Fig. 5A). Notably, the EPA group exhibited enrichment of several taxa, including *f_Brevibacteriaceae*, *f_Dermabacteraceae*, *f_Dietziaceae*, *f_Bradyrhizobiaceae*, *f_Methylobacteriaceae*, *f_Akkermansiaceae*, *o_Verrucomicrobiales*, and *c_Verrucomicrobiia* (Fig. 5A).

Additionally, functional profiling of the gut microbiota revealed group-specific differences in microbial metabolic potential (Fig. 5B). Analysis of KEGG level 2 pathways showed that EPA treatment modulated functional pathways, including those involved in carbohydrate metabolism and xenobiotic biodegradation and metabolism (Fig. 5B).

FMT Counteracts the Protective Effects of EPA in AS Mice

In the AS+EPA group, EPA therapy substantially alleviated vascular wall thickness and lesion severity in the aortic root (Fig. 6A). Consistently, Oil Red O staining demonstrated that EPA substantially suppressed lipid droplet accumulation within atherosclerotic plaques (Fig. 6B). However, FMT treatment counteracted these protective effects, restoring the severity of the lesions to levels comparable to those in the AS group (Fig. 6A,B).

Biochemical analyses showed that EPA treatment significantly reduced TC, TG, LDL-C, and ROS levels, while elevating HDL-C levels and mitochondrial membrane potential ($p < 0.01$, Fig. 6C–F and Fig. 7A–D). These beneficial outcomes were offset by FMT treatment ($p < 0.01$, Fig. 6C–F and Fig. 7A–D). Furthermore, efferocytosis in the aortic root of AS mice, which was enhanced by EPA, decreased after intragastric administration of FMT, as evidenced by a decrease in the number of ingested apoptotic cells ($p < 0.05$, Fig. 7E,F).

Discussion

This study demonstrated that EPA significantly ameliorated the pathological features of AS in mice. EPA treatment reduced serum levels of TC, TG, and LDL-C, while increasing HDL-C levels. Upregulation of TC, TG, and LDL-C is commonly associated with plaque formation, endothelial dysfunction, and inflammatory responses during the progression of AS [19]. In contrast, HDL-C exerts anti-inflammatory and antioxidant effects, promoting reverse cholesterol transport, contributing to preventing or even reversing atherosclerotic progression [20]. These findings suggest that EPA can effectively alleviate AS development by improving lipid metabolism and overall lipid profiles. Mitochondrial dysfunction is increasingly recognized as a critical contributor to the initiation and progression of AS, driven by loss of mitochondrial membrane potential, excessive ROS production, mitochondrial DNA damage, and metabolic disruptions [21]. Recent evidence indicates that macrophage-derived gasdermin D (GSDMD) forms pores in the mitochondrial membrane, leading to the release of mitochondrial DNA, inflammasome activation, and exacerbation of AS [22]. In contrast, approaches such as mitochondria-targeted delivery of esculetin have been found to suppress vascular senescence and inflammation, thereby attenuating AS [23]. Consistent with these find-

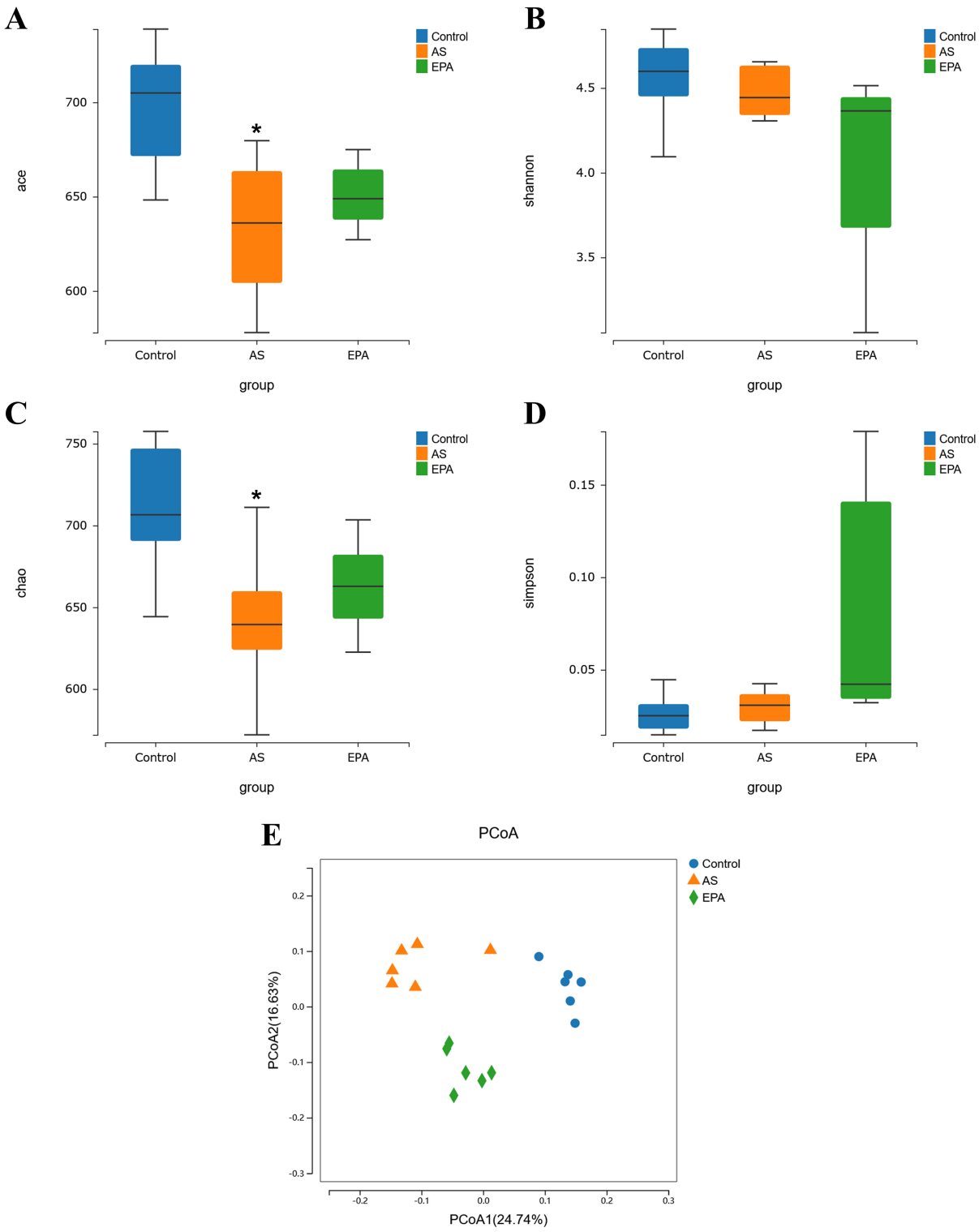

Fig. 3. Alpha and beta diversity analyses of gut microbiota. (A–D) Distribution of the ACE, Shannon, Chao, and Simpson indices in the Control, AS, and EPA groups. (E) Principal coordinate analysis (PCoA) plot illustrating beta diversity differences among the Control, AS, and EPA groups. $^{*}p < 0.05$ versus Control, n = 6 per group.

ings, our study revealed that EPA restored mitochondrial membrane potential and reduced ROS levels in the aortic tissues of AS mice, highlighting its potential role in improving mitochondrial function and alleviating AS progression.

Efferocytosis is a process by which phagocytes, such as macrophages, actively recognize, engulf, and degrade apoptotic cells, playing a crucial role in controlling the progression of AS [24]. The persistent accumulation of foam

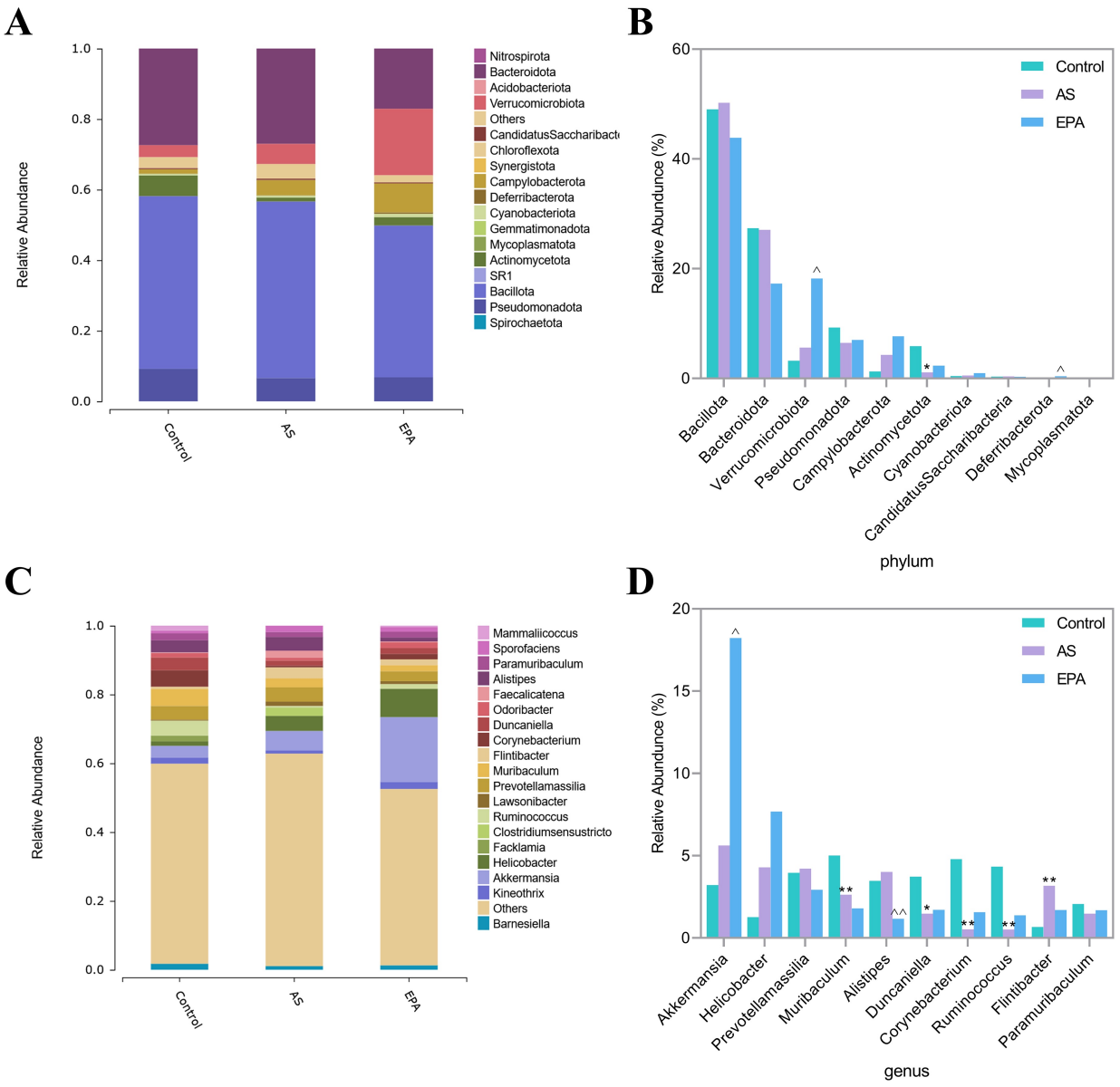

Fig. 4. Differences in gut microbiota composition at phylum and genus levels. (A,B) Stacked bar and bar plots showing the relative abundance of microbial communities at the phylum level in the Control, AS, and EPA groups. (C,D) Stacked bar and bar plots showing relative abundance at the genus level in the Control, AS, and EPA groups. n = 6 per group. $^{*}p < 0.05$, $^{**}p < 0.01$ versus Control; $^{\wedge}p < 0.05$, $^{\wedge\wedge}p < 0.01$ versus AS.

cells within atherosclerotic plaques often leads to extensive apoptosis [25]. If these apoptotic cells are not cleared in a timely manner, they undergo secondary necrosis, releasing damage-associated molecular patterns (DAMPs) that aggravate inflammation and increase plaque vulnerability [4]. Prior studies have reported that enhancing efferocytosis promotes the clearance of apoptotic foam cells, suppresses the release of pro-inflammatory mediators, and reduces immune-inflammatory responses, ultimately limiting AS progression and its complications [26,27]. In line with these observations, our study showed that EPA significantly promoted macrophage efferocytosis in the aortic root of AS mice, suggesting that EPA may alleviate inflammation by restoring macrophage function. Consistently, gut microbiota-derived metabolites have been reported to enhance efferocytic activity in lupus-prone male BWF1 mice [28], potentially affecting disease progression by modulating the immune microenvironment. These findings highlight the potential role of the gut-efferocytosis axis in the immunopathology of AS.

FMT, originally developed for recurrent Clostridioides difficile infections, has emerged as a promising strategy for restoring gut microbial homeostasis and regulating the host's immune-metabolic balance [29,30]. In re-

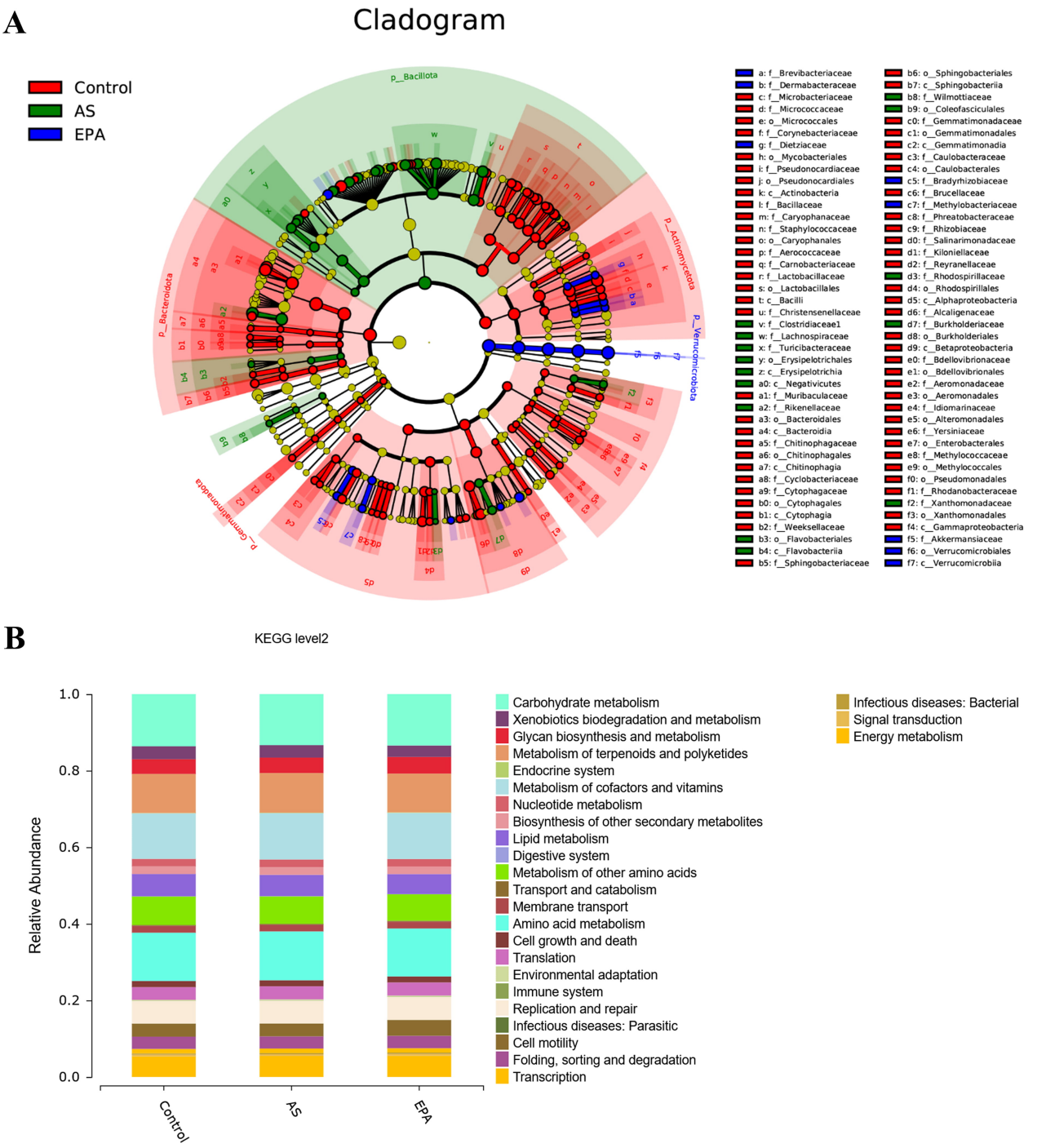

Fig. 5. Differential microbial taxa and functional pathway analysis. (A) Differentially abundant taxa among the Control, AS, and EPA groups across taxonomic levels were identified through Linear discriminant analysis effect size (LEfSe). (B) Functional profiling showing relative abundance of microbial metabolic pathways at Kyoto Encyclopedia of Genes and Genomes (KEGG) level 2. n = 6 per group.

cent years, its applications have expanded to treating diseases such as inflammatory bowel disease, metabolic disorders, cancer immunotherapy, and cardiovascular diseases, primarily by modulating microbial diversity, metabolite production, gut barrier integrity, and systemic immunity [31,32]. In our study, both AS and EPA treatments reduced microbial richness and diversity; however, EPA partially alleviated the decline in species richness caused by AS. Notably, FMT using fecal samples derived from untreated AS mice reversed the protective effects of EPA on mitochondrial membrane potential, ROS levels, efferocytosis, and aortic pathology. These findings indicate that the gut microbiota plays a key mediating or even determining role in the anti-atherosclerotic actions of EPA. Further-

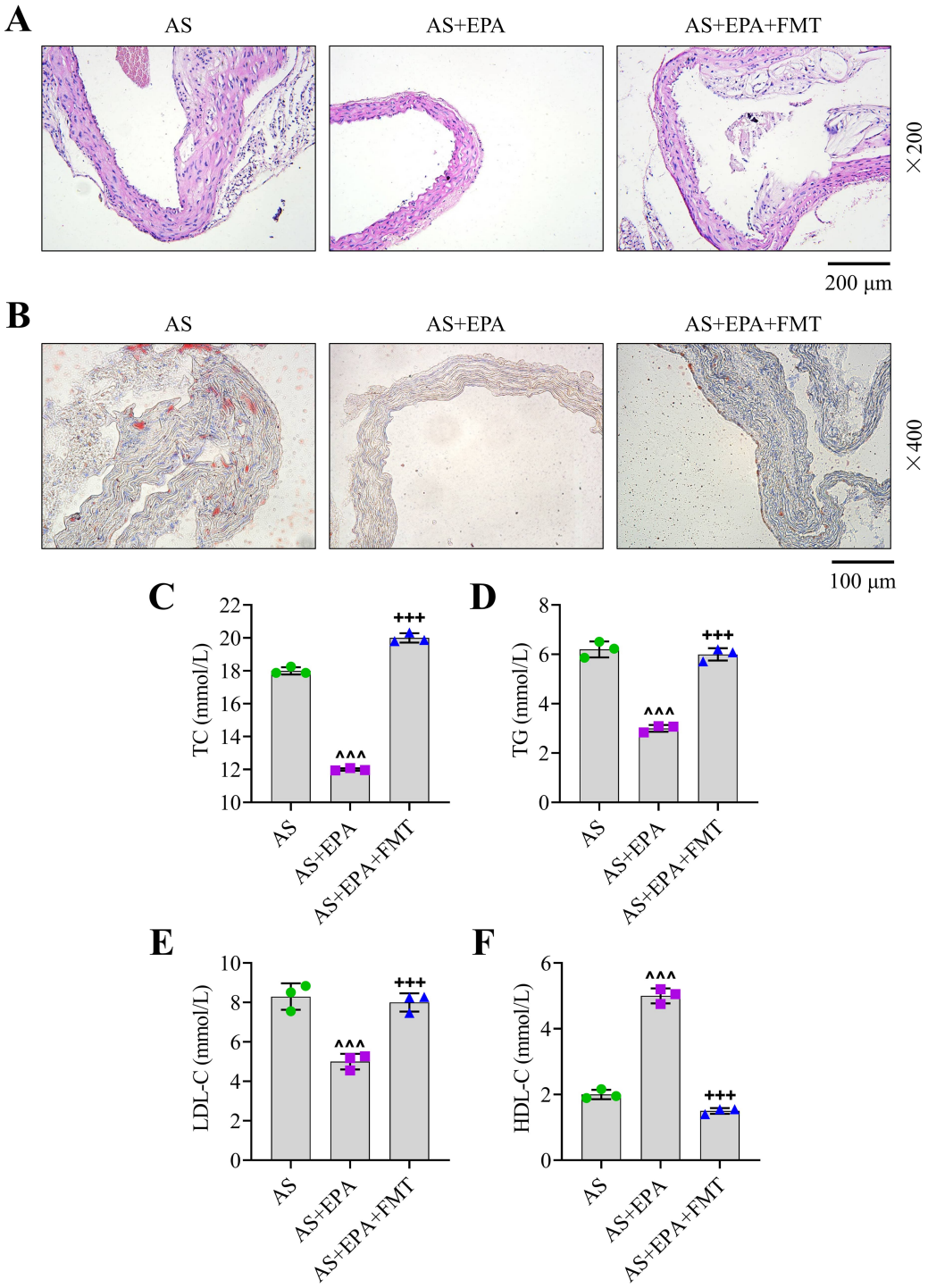

Fig. 6. Effects of EPA and fecal microbiota transplantation (FMT) on histopathological changes and lipid markers in AS. (A) H&E staining of the aortic roots from the AS, AS+EPA, and AS+EPA+FMT groups. Magnifications: 200×; scale bars: 200 μm. (B) Oil Red O staining of the aortic roots from the AS, AS+EPA, and AS+EPA+FMT groups. Magnifications: 400×; scale bars: 100 μm. (C–F) Serum TG, TC, HDL-C, and LDL-C levels in the AS, AS+EPA, and AS+EPA+FMT groups were determined using commercial kits. n = 3 per group. $^{\wedge\wedge\wedge}p < 0.001$ versus AS; $^{+++}p < 0.001$ versus AS+EPA.

more, they highlight the central role of the gut microbiota-mitochondria axis in regulating the pathophysiology of cardiovascular diseases.

The administration of probiotics has been shown to alleviate gut microbiota dysbiosis induced by high-calorie diets in mice by restoring microbial balance and increasing the abundance of beneficial bacteria (*Akkermansia*) [33,34].

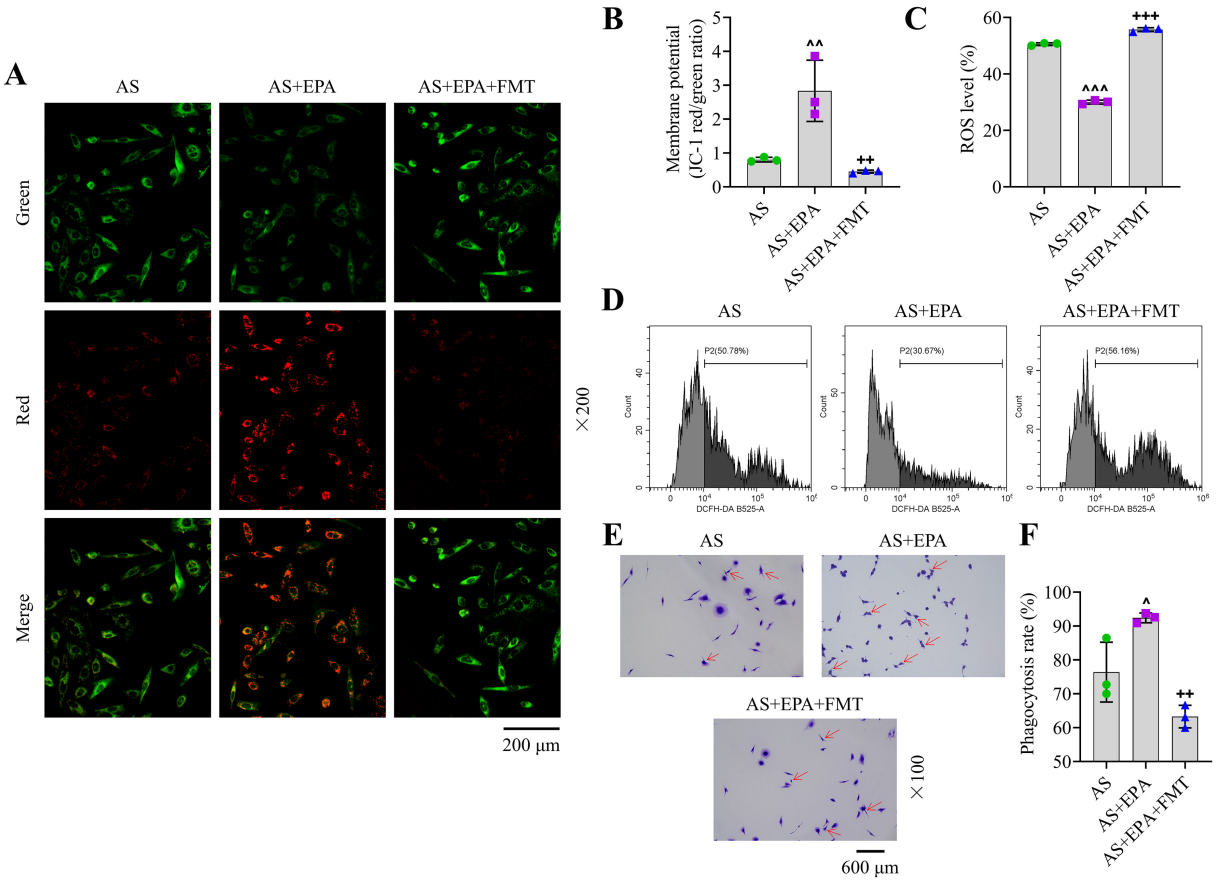

Fig. 7. Effects of EPA and FMT on mitochondrial function, ROS, and efferocytosis in AS. (A,B) JC-1 fluorescent probe assay to determine mitochondrial membrane potential in aortic cells from the AS, AS+EPA, and AS+EPA+FMT groups. Magnification: 200×; scale bar: 200 μm. (C,D) ROS levels were detected through DCFH-DA staining and flow cytometry in aortic cells from AS, AS+EPA, and AS+EPA+FMT groups. (E,F) Diff-Quick staining to assess efferocytosis in the aortic root of the AS, AS+EPA, and AS+EPA+FMT groups. Magnification: 100×; scale bar: 600 μm. n = 3 per group. $^{\wedge}p < 0.05$, $^{\wedge\wedge}p < 0.01$, $^{\wedge\wedge\wedge}p < 0.001$ versus AS; $^{+\!+}p < 0.01$, $^{+\!+\!+}p < 0.001$ versus AS+EPA.

Furthermore, clinical studies have reported that supplementation with pasteurized Akkermansia muciniphila in obese individuals significantly improves metabolic health, manifested as weight loss, lipid reduction, enhanced insulin sensitivity, and reduced inflammation, without adverse effects [35]. In our study, EPA treatment decreased TC, TG, and LDL-C levels while increasing the abundance of *Akkermansia*, indicating that EPA may enhance the gut through microbial remodeling. However, the role of *Akkermansia muciniphila* seems to be complex. Its membrane protein has been shown to inhibit colitis-associated tumors [36] and to reverse high-fat-diet-induced expression of pro-inflammatory factors (IL-6 and IL-1β) [37]. In contrast, some evidence suggests that *Akkermansia muciniphila* may trigger mitochondrial dysfunction in enteroendocrine cells, leading to calcium overload, ROS production, and α-synuclein aggregation [38].

Furthermore, unlike the above studies, some findings underscore a protective role, where *Akkermansia muciniphila* improves gut health and increases melatonin levels, providing antioxidant effects and enhancing mucosal repair against cadmium-induced damage by scavenging ROS and increasing goblet cell numbers [39]. Additionally, a recent study has shown that *Akkermansia muciniphila* significantly counteracts the high-fat-diet-induced mRNA expression levels of pro-inflammatory cytokines IL-6 and IL-1β. Furthermore, *Akkermansia muciniphila* is closely associated with SCFA formation [40], including propionic acid and butyric acid, which support intestinal homeostasis, are important metabolites produced by intestinal bacteria, promote regulatory T cell development, and influence cytokine secretion, such as IL-1, IL-6, and TNF-α [41]. Our results showed that although EPA increased *Akkermansia*, it also reduced ROS levels, indicating that EPA may regulate the gut-mitochondria axis through microbial remodeling, particularly through members of the *Akkermansiaceae* family. However, the precise roles of different bacterial genera in the gut-mitochondria interactions require further investigation.

Furthermore, research evidence has indicated that, compared with young adults, centenarians exhibit gut microbiota with higher microbial diversity, enhanced xenobiotic biodegradation and metabolism, increased oxidoreductases, and a higher abundance of certain species such as *Akkermansia* [42]. In our study, we found that xenobiotic biodegradation and metabolism pathways were involved and decreased after EPA treatment, while cell motility pathways were increased. However, neither AS nor EPA treatment caused significant changes in other functional structures of the microbial community. These observations suggest that different bacterial genera may compensate by performing the same functions, resulting in limited functional shift despite taxonomic alterations. Further experimental validation is needed to verify this hypothesis.

Despite certain promising outcomes, we acknowledge several limitations in this study. First, while we demonstrated the beneficial effects of EPA on mitochondrial function, efferocytosis, and AS progression, the precise molecular targets and signaling pathways involved remain to be elucidated. Second, although 16S rRNA gene sequencing provided a general overview of microbial composition, it lacked species-level resolution and comprehensive functional insight into the interaction between gut microbiota, mitochondrial function, and efferocytic activity. Additionally, the precise effects of FMT on gut microbiota remain unknown. Moreover, due to the lack of metabolite profiling and analysis of inflammatory cytokines, the complete causal chain linking gut microbiota, intermediary metabolites, and host functional impact could not be fully revealed. Finally, although mice from the same batch were used in our experiment, future investigations should consider using co-housed littermate mice to reduce inter-individual variability and increase experimental consistency.

Conclusion

In conclusion, this study reveals that EPA confers strong atheroprotective effects by remodeling the gut microbiota, restoring mitochondrial function, and enhancing efferocytosis. EPA treatment significantly reduces lipid accumulation, improves serum lipid profiles, restores mitochondrial membrane potential, suppresses ROS generation, and facilitates the clearance of apoptotic cells in the aortic root. 16S rRNA sequencing results confirm that EPA reshapes the gut microbial community and enriches beneficial microbial taxa. Importantly, fecal microbiota transplantation from untreated AS mice reverses these protective effects of EPA, underscoring the critical role of gut microbiota in mediating the therapeutic efficacy of EPA. Collectively, these findings not only advance our understanding of the multifaceted mechanisms of EPA but also identify the gut microbiota as a promising therapeutic target for managing AS.

Availability of Data and Materials

The analyzed data sets generated during the study are available from the corresponding author on reasonable request.

Author Contributions

YZ and SC designed the research study; SC performed the research; JL and DZ collected and analyzed the data. DZ has been involved in drafting the manuscript and all authors have been involved in revising it critically for important intellectual content. All authors give final approval of the version to be published. All authors have participated sufficiently in the work to take public responsibility for appropriate portions of the content and agreed to be accountable for all aspects of the work in ensuring that questions related to its accuracy or integrity are addressed.

Ethics Approval and Consent to Participate

All animal procedures were authorized by the Institutional Animal Care and Use Committee of Zhejiang Baiyue Biotechnology Co., Ltd. and carried out in compliance with the Guide for the Care and Use of Laboratory Animals (ZJBYLA-IACUC-20240715).

Acknowledgment

Not applicable.

Funding

This research was supported by the Ningbo Municipal Natural Science Foundation 2023 [grant numbers 2023J162].

Conflict of Interest

The authors declare no conflict of interest.

References

[1] Gusev E, Sarapultsev A. Atherosclerosis and Inflammation: Insights from the Theory of General Pathological Processes. International Journal of Molecular Sciences. 2023; 24: 7910. https://doi.org/10.3390/ijms24097910.

[2] Bethel M, Annex BH. Peripheral arterial disease: A small and large vessel problem. American Heart Journal Plus: Cardiology Research and Practice. 2023; 28: 100291. https://doi.org/10.1016/j.ahjo.2023.100291.

[3] Chen W, Li Z, Zhao Y, Chen Y, Huang R. Global and national burden of atherosclerosis from 1990 to 2019: trend analysis based on the Global Burden of Disease Study 2019. Chinese Medical Journal. 2023; 136: 2442–2450. https://doi.org/10.1097/CM9.0000000000002839.

[4] Zhang G, Li Q, Tao W, Qin P, Chen J, Yang H, *et al*. Sigma-1 receptor-regulated efferocytosis by infiltrating circulating macrophages/microglial cells protects against neuronal

impairments and promotes functional recovery in cerebral ischemic stroke. Theranostics. 2023; 13: 543–559. https://doi.org/10.7150/thno.77088.

[5] Doddapattar P, Dev R, Ghatge M, Patel RB, Jain M, Dhanesha N, *et al*. Myeloid Cell PKM2 Deletion Enhances Efferocytosis and Reduces Atherosclerosis. Circulation Research. 2022; 130: 1289–1305. https://doi.org/10.1161/CIRCRESAHA.121.320704.

[6] Liu WT, Li CQ, Fu AN, Yang HT, Xie YX, Yao H, *et al*. Therapeutic implication of targeting mitochondrial drugs designed for efferocytosis dysfunction. Journal of Drug Targeting. 2024; 32: 1169–1185. https://doi.org/10.1080/1061186X.2024.2386620.

[7] Kirichenko TV, Markina YV, Sukhorukov VN, Khotina VA, Wu WK, Orekhov AN. A Novel Insight at Atherogenesis: The Role of Microbiome. Frontiers in Cell and Developmental Biology. 2020; 8: 586189. https://doi.org/10.3389/fcell.2020.586189.

[8] Chen W, Zhang S, Wu J, Ye T, Wang S, Wang P, *et al*. Butyrate-producing bacteria and the gut-heart axis in atherosclerosis. Clinica Chimica Acta. 2020; 507: 236–241. https://doi.org/10.1016/j.cca.2020.04.037.

[9] Wang Z, Zhao Y. Gut microbiota derived metabolites in cardiovascular health and disease. Protein & Cell. 2018; 9: 416–431. https://doi.org/10.1007/s13238-018-0549-0.

[10] Zhang SJ, Li ZH, Zhang YD, Chen J, Li Y, Wu FQ, *et al*. Ketone Body 3-Hydroxybutyrate Ameliorates Atherosclerosis via Receptor Gpr109a-Mediated Calcium Influx. Advanced Science. 2021; 8: 2003410. https://doi.org/10.1002/advs.202003410.

[11] Seth J, Sharma S, Leong CJ, Rabkin SW. Eicosapentaenoic Acid (EPA) and Docosahexaenoic Acid (DHA) Ameliorate Heart Failure through Reductions in Oxidative Stress: A Systematic Review and Meta-Analysis. Antioxidants. 2024; 13: 955. https://doi.org/10.3390/antiox13080955.

[12] Ishida T, Naoe S, Nakakuki M, Kawano H, Imada K. Eicosapentaenoic Acid Prevents Saturated Fatty Acid-Induced Vascular Endothelial Dysfunction: Involvement of Long-Chain Acyl-CoA Synthetase. Journal of Atherosclerosis and Thrombosis. 2015; 22: 1172–1185. https://doi.org/10.5551/jat.28167.

[13] Libreros S, Shay AE, Nshimiyimana R, Fichtner D, Martin MJ, Wourms N, *et al*. A New E-Series Resolvin: RvE4 Stereochemistry and Function in Efferocytosis of Inflammation-Resolution. Frontiers in Immunology. 2021; 11: 631319. https://doi.org/10.3389/fimmu.2020.631319.

[14] Fu Y, Wang Y, Gao H, Li D, Jiang R, Ge L, *et al*. Associations among Dietary Omega-3 Polyunsaturated Fatty Acids, the Gut Microbiota, and Intestinal Immunity. Mediators of Inflammation. 2021; 2021: 8879227. https://doi.org/10.1155/2021/8879227.

[15] Ding L, Zhang LY, Shi HH, Wang CC, Jiang XM, Xue CH, *et al*. Eicosapentaenoic Acid-Enriched Phosphoethanolamine Plasmalogens Alleviated Atherosclerosis by Remodeling Gut Microbiota to Regulate Bile Acid Metabolism in LDLR$^{-/-}$ Mice. Journal of Agricultural and Food Chemistry. 2020; 68: 5339–5348. https://doi.org/10.1021/acs.jafc.9b08296.

[16] Zeng J, Deng Z, Zou Y, Liu C, Fu H, Gu Y, *et al*. Theaflavin alleviates oxidative injury and atherosclerosis progress via activating microRNA-24-mediated Nrf2/HO-1 signal. Phytotherapy Research. 2021; 35: 3418–3427. https://doi.org/10.1002/ptr.7064.

[17] Takashima A, Fukuda D, Tanaka K, Higashikuni Y, Hirata Y, Nishimoto S, *et al*. Combination of n-3 polyunsaturated fatty acids reduces atherogenesis in apolipoprotein E-deficient mice by inhibiting macrophage activation. Atherosclerosis. 2016; 254: 142–150. https://doi.org/10.1016/j.atherosclerosis.2016.10.002.

[18] Gan G, Zhang R, Zeng Y, Lu B, Luo Y, Chen S, *et al*. Fecal microbiota transplantation validates the importance of gut microbiota in an ApoE$^{-/-}$ mouse model of chronic apical periodontitis-induced atherosclerosis. BMC Oral Health. 2024; 24: 1455. https://doi.org/10.1186/s12903-024-05230-5.

[19] Du J, Ren Y, Liu J, Li T, Zhang Y, Yang S, *et al*. Association of Prolonged Disease Duration and TG/HDL-C Ratio in Accelerating Atherosclerosis in Patients with Takayasu's Arteritis. Clinical and Applied Thrombosis/Hemostasis. 2022; 28: 10760296221121297. https://doi.org/10.1177/10760296221121297.

[20] Bhale AS, Meilhac O, d'Hellencourt CL, Vijayalakshmi MA, Venkataraman K. Cholesterol transport and beyond: Illuminating the versatile functions of HDL apolipoproteins through structural insights and functional implications. BioFactors. 2024; 50: 922–956. https://doi.org/10.1002/biof.2057.

[21] Zong Y, Li H, Liao P, Chen L, Pan Y, Zheng Y, *et al*. Mitochondrial dysfunction: mechanisms and advances in therapy. Signal Transduction and Targeted Therapy. 2024; 9: 124. https://doi.org/10.1038/s41392-024-01839-8.

[22] Fan X, Han J, Zhong L, Zheng W, Shao R, Zhang Y, *et al*. Macrophage-Derived GSDMD Plays an Essential Role in Atherosclerosis and Cross Talk Between Macrophages via the Mitochondria-STING-IRF3/NF-κB Axis. Arteriosclerosis, Thrombosis, and Vascular Biology. 2024; 44: 1365–1378. https://doi.org/10.1161/ATVBAHA.123.320612.

[23] Singuru G, Pulipaka S, Shaikh A, Sahoo S, Jangam A, Thennati R, *et al*. Mitochondria targeted esculetin administration improves insulin resistance and hyperglycemia-induced atherosclerosis in db/db mice. Journal of Molecular Medicine. 2024; 102: 927–945. https://doi.org/10.1007/s00109-024-02449-1.

[24] Mehrotra P, Ravichandran KS. Drugging the efferocytosis process: concepts and opportunities. Nature Reviews. Drug Discovery. 2022; 21: 601–620. https://doi.org/10.1038/s41573-022-00470-y.

[25] Gui Y, Zheng H, Cao RY. Foam Cells in Atherosclerosis: Novel Insights Into Its Origins, Consequences, and Molecular Mechanisms. Frontiers in Cardiovascular Medicine. 2022; 9: 845942. https://doi.org/10.3389/fcvm.2022.845942.

[26] Tang C, Wang H, Guo L, Cui Y, Zou C, Hu J, *et al*. Multifunctional Nanomedicine for Targeted Atherosclerosis Therapy: Activating Plaque Clearance Cascade and Suppressing Inflammation. ACS Nano. 2025; 19: 3339–3361. https://doi.org/10.1021/acsnano.4c12131.

[27] Rochette L, Dogon G, Rigal E, Zeller M, Cottin Y, Vergely C. Interplay between efferocytosis and atherosclerosis. Archives of Cardiovascular Diseases. 2023; 116: 474–484. https://doi.org/10.1016/j.acvd.2023.07.007.

[28] Harder JW, Ma J, Alard P, Sokoloski KJ, Mathiowitz E, Furtado S, *et al*. Male microbiota-associated metabolite restores macrophage efferocytosis in female lupus-prone mice via activation of PPARγ/LXR signaling pathways. Journal of Leukocyte Biology. 2023; 113: 41–57. https://doi.org/10.1093/jleuko/qiac002.

[29] Porcari S, Benech N, Valles-Colomer M, Segata N, Gasbarrini A, Cammarota G, *et al*. Key determinants of success in fecal microbiota transplantation: From microbiome to clinic. Cell Host & Microbe. 2023; 31: 712–733. https://doi.org/10.1016/j.chom.2023.03.020.

[30] Kim ES, Yoon BH, Lee SM, Choi M, Kim EH, Lee BW, *et al*. Fecal microbiota transplantation ameliorates atherosclerosis in mice with C1q/TNF-related protein 9 genetic deficiency. Experimental & Molecular Medicine. 2022; 54: 103–114. https://doi.org/10.1038/s12276-022-00728-w.

[31] Fan L, Ren J, Chen Y, Wang Y, Guo Z, Bu P, *et al*. Effect of fecal microbiota transplantation on primary hypertension and the underlying mechanism of gut microbiome restoration: protocol

of a randomized, blinded, placebo-controlled study. Trials. 2022; 23: 178. https://doi.org/10.1186/s13063-022-06086-2.

[32] Antushevich H. Fecal microbiota transplantation in disease therapy. Clinica Chimica Acta. 2020; 503: 90–98. https://doi.org/10.1016/j.cca.2019.12.010.

[33] Kong C, Gao R, Yan X, Huang L, Qin H. Probiotics improve gut microbiota dysbiosis in obese mice fed a high-fat or high-sucrose diet. Nutrition. 2019; 60: 175–184. https://doi.org/10.1016/j.nut.2018.10.002.

[34] Cani PD, Depommier C, Derrien M, Everard A, de Vos WM. Akkermansia muciniphila: paradigm for next-generation beneficial microorganisms. Nature Reviews. Gastroenterology & Hepatology. 2022; 19: 625–637. https://doi.org/10.1038/s41575-022-00631-9.

[35] Depommier C, Everard A, Druart C, Plovier H, Van Hul M, Vieira-Silva S, *et al*. Supplementation with Akkermansia muciniphila in overweight and obese human volunteers: a proof-of-concept exploratory study. Nature Medicine. 2019; 25: 1096–1103. https://doi.org/10.1038/s41591-019-0495-2.

[36] Wang L, Tang L, Feng Y, Zhao S, Han M, Zhang C, *et al*. A purified membrane protein from *Akkermansia muciniphila* or the pasteurised bacterium blunts colitis associated tumourigenesis by modulation of $CD8^+$ T cells in mice. Gut. 2020; 69: 1988–1997. https://doi.org/10.1136/gutjnl-2019-320105.

[37] Shin NR, Lee JC, Lee HY, Kim MS, Whon TW, Lee MS, *et al*. An increase in the Akkermansia spp. population induced by metformin treatment improves glucose homeostasis in diet-induced obese mice. Gut. 2014; 63: 727–735. https://doi.org/10.1136/gutjnl-2012-303839.

[38] Amorim Neto DP, Bosque BP, Pereira de Godoy JV, Rodrigues PV, Meneses DD, Tostes K, *et al*. *Akkermansia muciniphila* induces mitochondrial calcium overload and α -synuclein aggregation in an enteroendocrine cell line. iScience. 2022; 25: 103908. https://doi.org/10.1016/j.isci.2022.103908.

[39] Xie S, Zhang R, Li Z, Liu C, Xiang W, Lu Q, *et al*. Indispensable role of melatonin, a scavenger of reactive oxygen species (ROS), in the protective effect of Akkermansia muciniphila in cadmium-induced intestinal mucosal damage. Free Radical Biology & Medicine. 2022; 193: 447–458. https://doi.org/10.1016/j.freeradbiomed.2022.10.316.

[40] Wu Z, Huang S, Li T, Li N, Han D, Zhang B, *et al*. Gut microbiota from green tea polyphenol-dosed mice improves intestinal epithelial homeostasis and ameliorates experimental colitis. Microbiome. 2021; 9: 184. https://doi.org/10.1186/s40168-021-01115-9.

[41] Deleu S, Machiels K, Raes J, Verbeke K, Vermeire S. Short chain fatty acids and its producing organisms: An overlooked therapy for IBD? eBioMedicine. 2021; 66: 103293. https://doi.org/10.1016/j.ebiom.2021.103293.

[42] Wu L, Xie X, Li Y, Liang T, Zhong H, Yang L, *et al*. Gut microbiota as an antioxidant system in centenarians associated with high antioxidant activities of gut-resident Lactobacillus. NPJ Biofilms and Microbiomes. 2022; 8: 102. https://doi.org/10.1038/s41522-022-00366-0.